ChemComm
Chemical Communications

Accepted Manuscript

This article can be cited before page numbers have been issued, to do this please use: C. Zhao, N. Zhu, G. Xu, R. Wang, T. Zhu, J. Tan and X. Gu, *Chem. Commun.*, 2020, DOI: 10.1039/D0CC00494D.

ROYAL SOCIETY OF CHEMISTRY

rsc.li/chemcomm

View Article Online
DOI: 10.1039/D0CC00494D

COMMUNICATION

Precise imaging of mitochondria in cancer cells by real-time monitoring nitroreductase activity with a targetable and activatable fluorescent probe

Received 00th January 20xx,
Accepted 00th January 20xx

DOI: 10.1039/x0xx00000x

Ning Zhu,[a,§] Ge Xu,[a,§] Rongchen Wang,[a] Tianli Zhu,[a] Jiahui Tan,[b] Xianfeng Gu,*[b] Chunchang Zhao *[a]

An activatable and mitochondrial-targetable fluorescent probe was developed. This designed probe showed ratiometric fluorescence and light-up near-infrared emission responsiveness to nitroreductase, achieving precise imaging of mitochondria in cancer cells by real-time monitoring nitroreductase activity.

Mitochondrion, a well-known energizing organelle in mammalian cells, provides the energy required for cell operation by generating ATP.[1] Mitochondria are widely involved in various cell processes, including signal transduction, energy metabolism, autophagy and apoptosis.[2] Accordingly, these cellular organelles are of vital importance in maintaining the normal physiological functions of organisms.[3] Meanwhile, mitochondrial function damage is also closely related to the occurrence of various diseases such as cancer, cardiovascular disease and dementia.[4] Therefore, it's of physiological and biological scientific interests for accurate imaging of mitochondria and real-time monitoring of substances closely related to mitochondrial function in cells.[5] Until now, fluorescence imaging has attracted wide attention to mitochondrial imaging due to its advantages such as high sensitivity, high spatio-temporal resolution and simple operation.[6] However, most of the available mitochondrial-targeted fluorescent probes are always-on, endowing poor specificity and thus incapable of specific imaging of mitochondria in cancer cells.[7] Therefore, the accurate imaging of mitochondrial in cancer cells remains a big challenge.

Activatable probes have been extensively explored in recent years for targeting cancer cells imaging.[8] Compared with conventional nonresponsive probes, activatable fluorescent probes can switch on fluorescence that is distinguished from the original state only after specific activation by biological targets.[9] Therefore, activatable fluorescent probes usually have high selectivity and low background interference, which is suitable for accurate detection of biological targets *in vivo*.[10] In this regard, we attended to design an activatable fluorescent probe with a mitochondrial-targeted group, which can be selectively activated by enzymes overexpressed in the cancer cells, aiming at imaging of mitochondria in cancer cells with high precision.

Herein, we developed a mitochondria-targetable fluorescent probe (BOD-TPP) that showed selective response to nitroreductase. Such a probe was designed by linking p-nitrobenzyl thioether and triphenylphosphine to the parent boron dipyrromethene (BODIPY) platform (Scheme 1).[11] Triphenylphosphine, a lipophilic cation, could specifically target to the mitochondria.[12] P-nitrobenzyl thioether could be reduced to p-aminobenzyl thioether by nitroreductase (NTR), followed by a 1,6-elimination reaction to release the required fluorophore, showing advantages of dual-channel ratiometric fluorescence and light-up near-infrared emission. As is well-known, nitroreductase, a type of flavin-containing enzymes overexpressed in cancer cells can be considered as a biomarker for cancers.[13] Accordingly, this designed probe enabled highly accurate imaging of mitochondria in cancer cells by real-time monitoring nitroreductase activity.

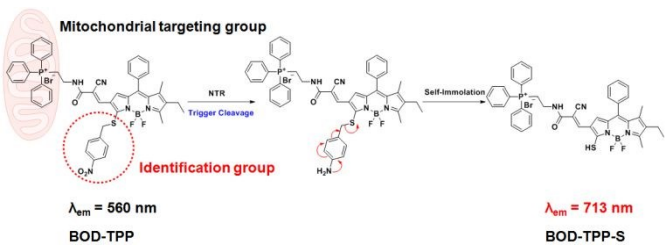

Scheme 1 Schematic illustration of BOD-TPP and the mechanism for nitroreductase (NTR)-activated ratiometric and NIR fluorescence light up.

[a] *Key Laboratory for Advanced Materials and Feringa Nobel Prize Scientist Joint Research Center, Institute of Fine Chemicals, School of Chemistry and Molecular Engineering, East China University of Science and Technology, Shanghai, 200237, P. R. China. Email Address: zhaocchang@ecust.edu.cn*
[b] *Department of Medicinal Chemistry, School of Pharmacy, Fudan University, Shanghai, 201203, P. R. China. Email Address: xfgu@fudan.edu.cn*
§ These authors contributed equally.
† Footnotes relating to the title and/or authors should appear here.
Electronic Supplementary Information (ESI) available: [details of any supplementary information available should be included here]. See DOI: 10.1039/x0xx00000x

BOD-TPP was readily synthesized and purified by column chromatography (Scheme 2). The detailed synthetic steps were described in Scheme S1 (ESI†). Next the response of BOD-TPP toward nitroreductase was evaluated under model conditions (DMSO/Tris-HCl buffer, 1/3, v/v, 0.05 M, pH 7.4, 37 °C) by monitoring changes in the absorption and emission spectra. Here, dimethyl sulfoxide was selected as a cosolvent to improve the aqueous solubility of the probe. As expected, BOD-TPP showed obvious responsiveness to nitroreductase. In the absence of nitroreductase, BOD-TPP exhibited an intense absorption at 495 nm and an emission band at 560 nm (fluorescence quantum yield ϕ of 17.8%). Upon addition of NADH (500 μM) and nitroreductase (10 μg/mL), a new absorption band appeared at 650 nm, and the original 495 nm absorption band decreased concomitantly (Fig. 1a), showing a big red-shift of 155 nm. Interestingly, the fluorescence titration experiments showed that BOD-TPP can measure nitroreductase in both dual-channel ratiometric and turn-on near-infrared fluorescence modes. The presence of nitroreductase led to the quenching of the fluorescence at 560 nm upon excitation at 495 nm, while a new near-infrared emission at 713 nm was activated when the excitation wavelength was 650 nm (Fig. 1c). These changes were ascribed to the successful conversion of BOD-TPP to BOD-TPP-S (ϕ of 5.3%) by nitroreductase that could trigger a cascade reactions including the formation of the p-aminobenzyl thioether linker and a subsequent 1,6-elimination reaction to release the required fluorophore. This mechanism could be confirmed by High-resolution mass spectrometry (HRMS) analysis (Fig. S1, ESI†). As shown in Fig. S1, HRMS spectrum of BOD-TPP solution in the presence of NTR gave peaks of 739.2641 (corresponding to [BOD-TPP-S - Br]$^+$) and 874.2972 (corresponding to [BOD-TPP - Br]$^+$). In the buffer solution at pH 7.4, the kinetics values of BOD-TPP against nitroreductase showed that Michaelis-Menten constant (K_m) was 33.70 μM and V_{max} was 46.21 μM · min^{-1} (Fig. S3, ESI†). Importantly, a linear relationship between the fluorescence intensity and nitroreductase concentration was noted in the measured range of 0 μg/mL to 10 μg/mL, affording the detection limit of 0.0168 μg/mL (Fig. S4, ESI†).

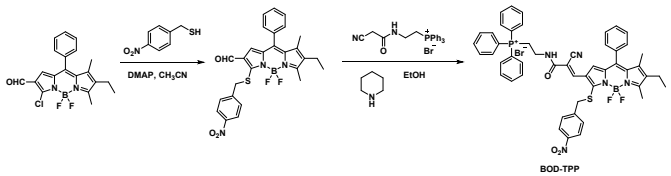

Scheme 2 Synthetic route of BOD-TPP.

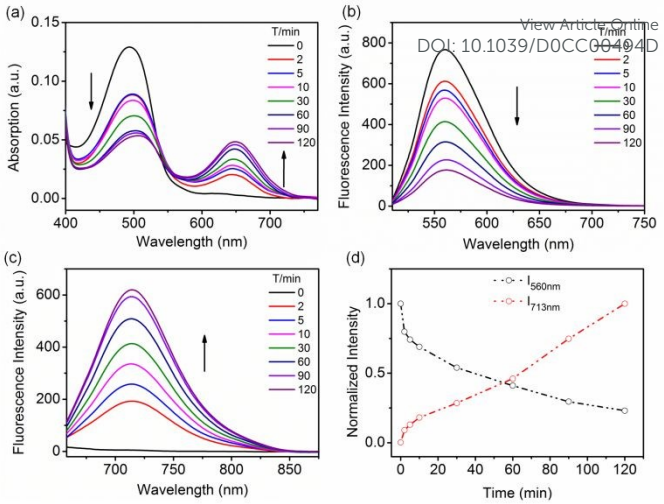

Fig. 1 Time-dependent spectral changes of BOD-TPP (10 μM) in the presence of nitroreductase (NTR) (10 μg/mL). (a) Absorption, (b) fluorescence quenching (λ_{ex} = 495 nm) and (c) fluorescence turn-on (λ_{ex} = 650 nm) in buffer (DMSO/Tris-HCl buffer, 1/3, v/v, 0.05 M, pH 7.4) at 37 °C. (d) Time-dependent fluorescence intensity of I_{560nm} and I_{713nm}.

BOD-TPP showed highly selective response to nitroreductase. As shown in Figure 2a and Figure S5 (ESI†), interfering species including other enzymes and thiols caused negligible fluorescence changes, whereas the introduction of NADH and nitroreductase caused a significant increase in fluorescence intensity at 713 nm. It was worth noting that negligible fluorescence enhancement was found upon pretreatment of nitroreductase with an inhibitor dicoumarol (Fig. 2b), suggesting that nitroreductase played a key role in activation of BOD-TPP. This further illustrated that BOD-TPP unambiguously exhibited high specificity for nitroreductase activity. In addition, the probe exhibited good optical responsiveness to enzyme in the physiological pH range (pH 8.5 to approximately 6; Fig. S6, ESI†).

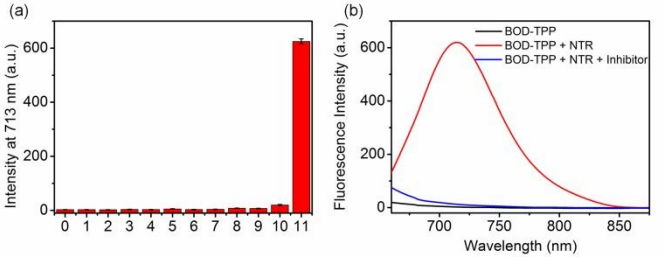

Fig. 2 (a) The fluorescence intensity at 713 nm of BOD-TPP (10 μM) in the presence of nitroreductase (NTR) and other biologically related analytes were incubated in buffer (DMSO/Tris-HCl buffer, 1/3, v/v, 0.05 M, pH 7.4) at 37 °C for 120 min: (0) Free; (1) aprotinin (30 μg/mL); (2) phosphatase (30 μg/mL); (3) collagenase (30 μg/mL); (4) lipase (30 μg/mL); (5) BSA (10 mg/mL); (6) NQO1 (30 μg/mL); (7) NADH (500 μM); (8) GSH (1 mM); (9) Cys (1 mM); (10) Hcy (1 mM); (11) NADH (500 μM) + NTR (10 μg/mL). (b) NTR-induced the fluorescence enhancement of BOD-TPP in the absence or presence of inhibitor dicoumarol (0.2 mM).

The low cytotoxicity of BOD-TPP to living cells was demonstrated through CCK-8 experiment (Fig. S7, ESI†). Then we testified its ability to selectively identify cancer cells by tracking enzyme activity in real time. In order to testify the feasibility of visualization of cancer cells based on nitroreductase activity, imaging experiments were performed on A549 cells (high nitroreductase activity).[13a] As shown in Fig. 3a-3c, the fluorescence ratio (I_{red}/I_{green}) of BOD-TPP-stained A549 cells showed a time-dependent enhancement. Obviously, the fluorescence signals in the green channel was continuously attenuated as prolonging the incubation time, while the signals in red channel progressively increased, resulting in the change of I_{red}/I_{green} from 0.08 to 5.5. On the contrary, pretreatment of the cells with the enzyme inhibitor dicoumarol significantly lowered the ratio of I_{red}/I_{green} due to the suppression of the nitroreductase activity (Fig. 3d), which further indicated that fluorescence imaging signals were indeed initiated by nitroreductase activity.

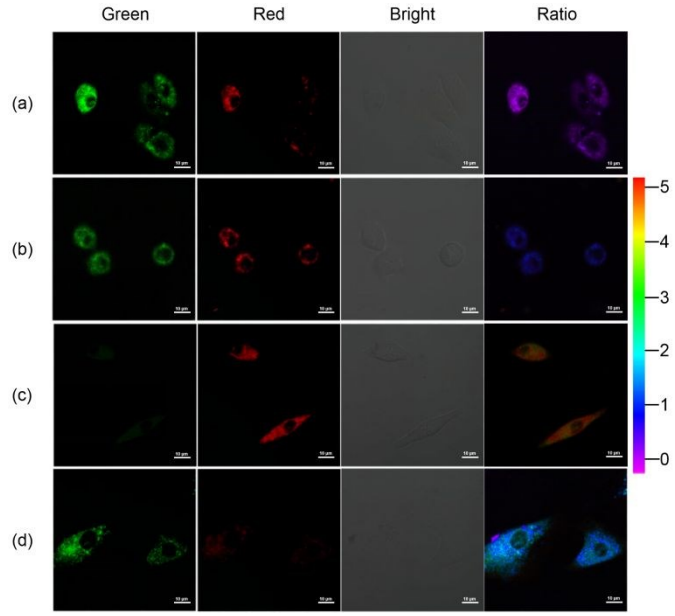

Fig. 3 Visualization of A549 cells by confocal microscopy imaging. A549 cells incubated with BOD-TPP (10 μM) for (a) 15 min; (b) 30 min and (c) 60 min. (d) A549 cells pretreated with dicoumarol (0.5 mM) for 60 min, followed by treatment with BOD-TPP (10 μM) for 60 min. Green channel at 525–600 nm with λ_{ex} = 488 nm excitation, red channel at 675–750 nm using λ_{ex} = 561 nm; ratio image was I_{red} /I_{green}. Scale bar = 10 μm.

To further investigate the subcellular localization of the probe, a widely used commercial mitochondrial targeting dye Mito-Tracker Green was used for colocalization study. As shown in Fig. 4, the results clearly showed the red signal was generated by the probe, and the green channel illustrated visualization of mitochondria by Mito-Tracker Green. Superposition of panels a-c showed complete overlap of the red and green signals. Pearson's colocalization coefficient, which used to describe the correlation of the intensity distribution between the two channels, was caculated to be 0.96 (Fig. 4). All these results confirmed that the probe we designed could be specifically localized in the mitochondria of living A549 cells. Notably, the common nitroreductase probes are known to imaging nitroreductase activity in hypoxic tumor cells, while few probe show selective monitoring of nitroreductase under normoxic conditions.[13] The selective responsiveness of this probe to nitroreductase in normoxic tumor cells might enable the accurate imaging of the mitochondria in cancer cells.

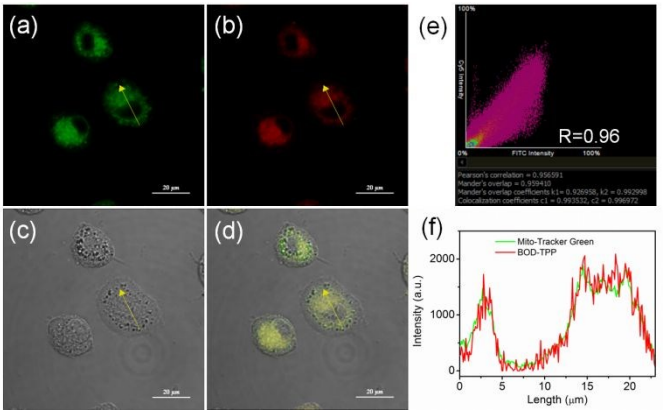

Fig. 4 Fluorescence emission from BOD-TPP colocalized to mitochondria in live A549 cells. (a) A549 cells were incubated with Mito-Tracker Green (50 nM) for 30 min. (b) A549 cells were incubated with BOD-TPP (10 μM) for 60 min. (c) Bright field. (d) Overlay of images a–c. (e) Pearson's colocalization coefficient. (f) The intensity profile showed the fluorescence intensity along the yellow line across the cell. Scale bar = 20 μm.

In summary, we have developed a novel activatable BODIPY-based NIR fluorescent probe for monitoring of nitroreductase activity and imaging of mitochondria in cancer cells. This activatable probe was designed by appending p-nitrobenzyl thioether and triphenylphosphine function to the parent BODIPY platform. Nitroreductase could trigger the formation of the p-aminobenzyl thioether linker that was capable of undergoing a 1,6-elimination reaction to release a NIR fluorophore, enabling selective detection of nitroreductase. In light of the mitochondria targetable feature, ratiometric fluorescence and NIR emission light-up responsiveness to nitroreductase, our probe achieved high-precision imaging of mitochondria in cancer cells by real-time monitoring nitroreductase activity. We expect that our design approach could have more applications in nitroreductase-based biology or mitochondrial biology.

We gratefully acknowledge the financial support by the National Natural Science Foundation of China (21874043, 21672062, 21977018), the Shanghai Municipal Science and Technology Major Project (Grant No. 2018SHZDZX03) and the Programme of Introducing Talents of Discipline to Universities (B16017).

Conflicts of interest

There are no conflicts to declare.

Notes and references

1 (a) P. Yuan, X. Mao, X. Wu, S. S. Liew, L. Li and S. Q. Yao, *Angew. Chem. Int. Ed.*, 2019, **58**, 7657; (b) X. Tan, S. Luo, L. Long, Y. Wang, D. Wang, S. Fang, Q. Ouyang, Y. Su, T. Cheng and C. Shi, *Adv. Mater.*, 2017, **29**, 1704196.

2 (a) Y. Zhang, Z. Li, W. Hu and Z. Liu, *Anal. Chem.*, 2019, **91**, 10302; (b) Y. Ni, H. Zhang, C. Chai, B. Peng, A. Zhao, J. Zhang, L. Li, C. Zhang, B. Ma, H. Bai, K. L. Lim and W. Huang, *Adv. Healthcare Mater.*, 2019, **8**. ,1900212.

3 (a) P. Ning, J. Jiang, L. Li, S. Wang, H. Yu, Y. Feng, M. Zhu, B. Zhang, H. Yin, Q. Guo and X. Meng, *Biosens. Bioelectron.*, 2016, **77**, 921; (b) K. Qiu, J. Wang, T. W. Rees, L. Ji, Q. Zhang and H. Chao, *Chem. Commun.*, 2018, **54**, 14108.

4 S. Luo, X. Tan, S. Fang, Y. Wang, T. Liu, X. Wang, Y. Yuan, H. Sun, Q. Qi and C. Shi, *Adv. Funct. Mater.*, 2016, **26**, 2826.

5 (a) Y. Zhu, K. Wang, W. Song, B. Dong, S. Zhao, R. Guan, Z. Li, Y. Sun, D. Cao and W. Lin, *Sens. Actuators B: Chem.*, 2019, **294**, 283; (b) J. Xu, J. Pan, X. Jiang, C. Qin, L. Zeng, H. Zhang and J. F. Zhang, *Biosens. Bioelectron.*, 2016, **77**, 725.

6 (a) X. Zhang, Q. Sun, Z. Huang, L. Huang and Y. Xiao, *J. Mater. Chem. B.*, 2019, **7**, 2749; (b) Y. Song, Y. Zheng, S. Zhang, Y. Song, M. Niu, Y. Li, Z. Ye, H. Yu, M. Zhang and Y. Xiao, *Sens. Actuators B: Chem.*, 2019, **286**, 32; (c) C. Zhang, H. Xie, T. Zhan, J. Zhang, B. Chen, Z. Qian, G. Zhang, W. Zhang and J. Zhou, *Chem. Commun.*, 2019, **55**, 9444.

7 (a) J. Zhang, Q. Wang, Z. Guo, S. Zhang, C. Yan, H. Tian and W. H. Zhu, *Adv. Funct. Mater.*, 2019, **29**, 1808155; (b) Z. Xu, M. X. Zhang, Y. Xu, S. H. Liu, L. Zeng, H. Chen and J. Yin, *Sens. Actuators B: Chem.*, 2019, **290**, 676.

8 (a) J. Li, F. Cheng, H. Huang, L. Li and J. Zhu, *Chem. Soc. Rev.*, 2015, **44**, 7855; (b) R. Wang, W. Gao, J. Gao, G. Xu, T. Zhu, X. Gu and C. Zhao, *Front. Chem.*, 2019, **7**, 778; (c) C. Zhao, X. Zhang, K. Li, S. Zhu, Z. Guo, L. Zhang, F. Wang, Q. Fei, S. Luo, P. Shi, H. Tian and W. H. Zhu, *J. Am. Chem. Soc.*, 2015, **137**, 8490; (d) Y. Liu, L. Teng, C. Xu, H. W. Liu, S. Xu, H. Guo, L. Yuan and X. B. Zhang, *Chem. Sci.*, 2019, **10**, 10931. (e) B. Shi, N. Ren, L. Gu, G. Xu, R. Wang, T. Zhu, Y. Zhu, C. Fan, C. Zhao and H. Tian, *Angew. Chem. Int. Ed.*, 2019, **58**, 16826.

View Article Online DOI: 10.1039/D0CC00494D

9 (a) B. Zhao, P. Wu, H. Zhang and C. Cai, *Biosens. Bioelectron.*, 2015, **68**, 763; (b) G. Xu, Q. Yan, X. Lv, Y. Zhu, K. Xin, B. Shi, R. Wang, J. Chen, W. Gao, P. Shi, C. Fan, C. Zhao and H. Tian, *Angew. Chem. Int. Ed.*, 2018, **57**, 3626. (c) G. Xu, W. Guo, X. Gu, Z. Wang, R. Wang, T. Zhu, H. Tian, C. Zhao, *CCS Chem.* 2020, **2**, 527.

10 (a) R. Wang, J. Chen, J. Gao, J. A. Chen, G. Xu, T. Zhu, X. Gu, Z. Guo, W. H. Zhu and C. Zhao, *Chem. Sci.*, 2019, **10**, 7222; (b) R. Wang, K. Dong, G. Xu, B. Shi, T. Zhu, P. Shi, Z. Guo, W. H. Zhu and C. Zhao, *Chem. Sci.*, 2019, **10**, 2785; (c) L. Y. Niu, Y. S. Guan, Y. Z. Chen, L. Z. Wu, C. H. Tung and Q. Z. Yang, *J. Am. Chem. Soc.*, 2012, **134**, 18928.

11 (a) J. Zhang, H. W. Liu, X. X. Hu, J. Li, L. H. Liang, X. B. Zhang and W. Tan, *Anal. Chem.*, 2015, **87**, 11832; (b) C. Zhao, J. An, L. Zhou, Q. Fei, F. Wang, J. Tan, B. Shi, R. Wang, Z. Guo and W. H. Zhu, *Chem. Commun.*, 2016, **52**, 2075; (c) C. Duan, M. Won, P. Verwilst, J. Xu, H. S. Kim, L. Zeng and J. S. Kim, *Anal. Chem.*, 2019, **91**, 4172.

12 (a) Roopa, N. Kumar, V. Bhalla and M. Kumar, *Chem. Commun.*, 2015, **51**, 15614; (b) J. Xu, F. Zeng, H. Wu and S. Wu, *J. Mater. Chem. B.*, 2015, **3**, 4904; (c) Z. Zhang, J. Fan, Y. Zhao, Y. Kang, J. Du and X. Peng, *ACS Sens.*, 2018, **3**, 735; (d) M. Gao, F. Yu, H. Chen and L. Chen, *Anal. Chem.*, 2015, **87**, 3631.

13 (a) A. Chevalier, Y. Zhang, O. M. Khdour, J. B. Kaye and S. M. Hecht, *J. Am. Chem. Soc.*, 2016, **138**, 12009; (b) B. Huang, W. Chen, Y. Q. Kuang, W. Liu, X. J. Liu, L. J. Tang and J. H. Jiang, *Org. Biomol. Chem.*, 2017, **15**, 4383; (c) J. Bae, L. McNamara, M. A. Nael, F. Mahdi, R. J. Doerksen, G. L. Bidwell, N. I. Hammer and S. Jo, *Chem. Commun.*, 2015, **51**, 12787; (d) R. H. F. Wong, T. Kwong, K. H. Yau and H. Y. Au-Yeung, *Chem. Commun.*, 2015, **51**, 4440; (e) Y. Li, Y. Sun, J. Li, Q. Su, W. Yuan, Y. Dai, C. Han, Q. Wang, W. Feng and F. Li, *J. Am. Chem. Soc.*, 2015, **137**, 6407.

View Article Online
DOI: 10.1039/D0CC00494D

COMMUNICATION

TOC

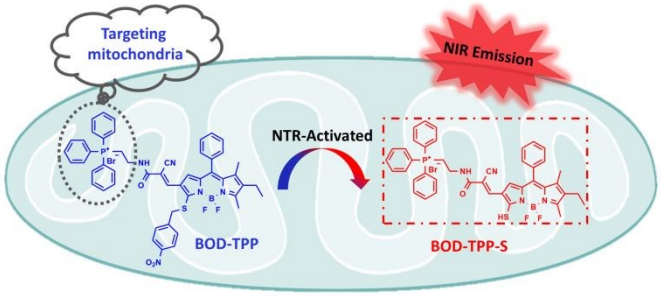

A probe with the mitochondria targetable feature and ratiometric fluorescence as well as NIR emission light-up responsiveness to nitroreductase is presented for precise imaging of **m**itochondria in cancer cells by real-time monitoring nitroreductase activity.